Band widening in graphite

C. Heske*
Advanced Light Source, Lawrence Berkeley National Laboratory, Berkeley, California 94720

R. Treusch† and F. J. Himpsel
Department of Physics, University of Wisconsin-Madison, Madison, Wisconsin 53706

S. Kakar
Department of Applied Science, University of California at Davis/Livermore, Livermore, California 94550

L. J. Terminello
Lawrence Livermore National Laboratory, Livermore, California 94550

H. J. Weyer
Swiss Light Source, Paul-Scherrer Institute, Villigen PSI, Switzerland

E. L. Shirley
National Institute of Standards and Technology, Optical Technology Division, Gaithersburg, Maryland 20899
(Received 15 May 1998)

The valence band width of graphite is determined with high accuracy by imaging the momentum distribution of photoelectrons for various binding energies. Compared to local-density-functional theory, the experimental band width (22.0 eV) is stretched by about 11%. Quasiparticle calculations, which properly describe electron interaction effects on the excited states of a solid, give a width of 21.8 eV, in agreement with the experiment within the experimental and theoretical relative uncertainty of about 1%. The results demonstrate the importance of including final-state and associated many-body effects into the theoretical description of the electronic structure of solids. [S0163-1829(99)11403-6]

Band calculations are at the foundation of understanding the electronic structure of solids. The most common theoretical method for obtaining energy bands and total energies of solids and surfaces is the local-density approximation (LDA).[1] This approach has been surprisingly successful for computing band dispersions, requiring very accurate band measurements to detect any systematic difference between LDA and experiment. This paper presents high-precision band structure measurements of graphite which test the limits of the local density approximation. We also go beyond this approximation by performing quasiparticle band calculations. In so doing, we also consider the many-body mechanisms (i.e., exchange and correlation or self-energy effects) which influence band energies.

Particular emphasis here is placed on the band width, because this is often considered the single most important quantity characterizing the valence band of a material. So far, rather few angle-resolved photoemission measurements have been performed with an accuracy of a few percent which is required to quantify the difference between measured and theoretical band widths. For a typical simple metal (Na) a band narrowing by 18% has been found relative to the LDA, and quasiparticle calculations suggest varying degrees of self-energy band narrowing.[2–4] For a prototype insulator (LiF) and wide-gap semiconductor (diamond), respectively, a 17 (Ref. 5) and 7% (Ref. 6) band widening compared to the LDA has been found in measurements and quasiparticle calculations.[7,8]

Graphite has traditionally been a test system for demonstrating the band-mapping capacity of angle-resolved photoemission. It is worthwhile, therefore, to consider this semimetal for study, particularly in view of the fact that the bandwidth discrepancy changes its sign from metals to semiconductors. Earlier experimental results for the valence band width in graphite vary significantly. Results from laboratory-based x-ray photoelectron spectroscopy (XPS) investigations of 24 eV$\pm$1 eV (Ref. 9) are different from band widths obtained with angle-resolved photoelectron spectroscopy (ARPES) at synchrotron sources. Bianconi *et al.* reported a width of 22.5 eV,[10] Eberhardt *et al.*, and McGovern *et al.* derived 20.6 eV$\pm$0.3 eV,[11] Law *et al.* found 21 eV and 22.3 eV$\pm$0.2 eV,[12] and Costanzo *et al.* reported widths of 20.5 eV for polygraphite and 21.0 eV for highly oriented pyrolytic graphite (HOPG).[13] In a recent electron momentum spectroscopy experiment, Vos *et al.* obtained a width of 21.5 to 22.5 eV.[14] Mirroring the large scatter in experimental values, theoretical results vary from 19.2 to 21.9 eV, with most of these results obtained using the LDA. While early LDA calculations indicated good agreement with some of the above experimental band widths (20.8, 21.5 eV),[15] recent results are generally below 20 eV, and full-potential results appear to be converging to around 19.6 eV.[16,17] In contrast, our theoretical investigation based on quasiparticle calculations derives a bandwidth of 21.8 eV$\pm$0.2 eV. Previous quasiparticle calculations by Zhu and Louie[18] indicate a similar value (21.5 eV).

We have performed an accurate valence band mapping of graphite at room temperature by employing an imaging photoelectron spectrometer,[19] which allows for a data rate orders of magnitude higher than was obtainable with single-angle spectrometers. A total of 5×10^6 image points were acquired at different angles, photon energies, and electron energies. The experiments were performed by utilizing the high flux and small spot size of the undulator Beamline 8.0 at the Advanced Light Source. A synthetic single-domain single crystal of Kish graphite provided by Takahashi was outgassed in vacuum at pressures in the 10^{-10} mbar range, and photoelectron momentum distribution images were taken for a set of 35 different binding energies throughout the valence band. Each of these images represents an isoenergetic slice through momentum space, i.e., shows an intensity distribution of emitted photoelectrons for a given binding energy, with different locations within an image being directly related to different values of $\mathbf{k}_\parallel$, the electron momentum parallel to the sample surface. For all images presented here, the detected electron kinetic energy was kept fixed at 130 eV and the incident photon energy was varied in order to probe electronic states with different binding energies. The overall energy resolution was determined to be better than 0.5 eV. A full width at half maximum (FWHM) analysis of the *K* points for binding energies close to the Fermi level yielded a conservative upper limit for the angular resolution of 1.6°, corresponding to a $\mathbf{k}_\parallel$ resolution of better than 0.1 Å^{-1}.

Figure 1 shows images for binding energies near prominent points of the graphite valence band structure. Features of high intensity are depicted as dark regions. In order to include the transmission of the analyzer, all images were normalized by an image of the secondary electron distribution at identical analyzer settings. A symmetrization of the images has been performed according to the threefold symmetry of the three-dimensional graphite crystal. All features in Fig. 1 were clearly visible in the unsymmetrized raw data. In particular, the valence band width reported here could be derived from both symmetrized and unsymmetrized images.

In detail, Fig. 1(a) shows the distribution pattern near the Fermi energy, for which the corners of the central hexagon define the position of the *K* points of the first (surface) Brillouin zone, where the π band intersects the Fermi level[20] (refer to Ref. 21 for a depiction of the two-dimensional graphite band structure). The *K* points in higher Brillouin zones are visible towards the edge of the image. Figure 1(b) was recorded near the top of the π band (at the *M* points) of the first Brillouin zone. Note that two of the points of highest intensity in the central ring (the *M* points) lie on a vertical line which includes Γ at the center of the image, whereas in Fig. 1(a) two of the highest intensity points (the *K* points) are found on a horizontal line. Figure 1(c) was recorded at a binding energy of 4.5 eV, just below the predicted top of the σ bands at Γ. As evident from the image, no central high-intensity feature is seen, the result of a Brillouin-zone selection effect.[21] Yet σ band emission intensity at Γ is observed in Fig. 1(c) in higher Brillouin zones (six Γ points near the edge of the image), consistent with the same selection rule. The central ring feature in Fig. 1(c) is ascribed to the π band, and it continues to decrease in diameter in Fig. 1(d) until it reaches its bottom at the Γ point at a binding energy close to that of Fig. 1(e). In Fig. 1(f), the intensity distribution shows

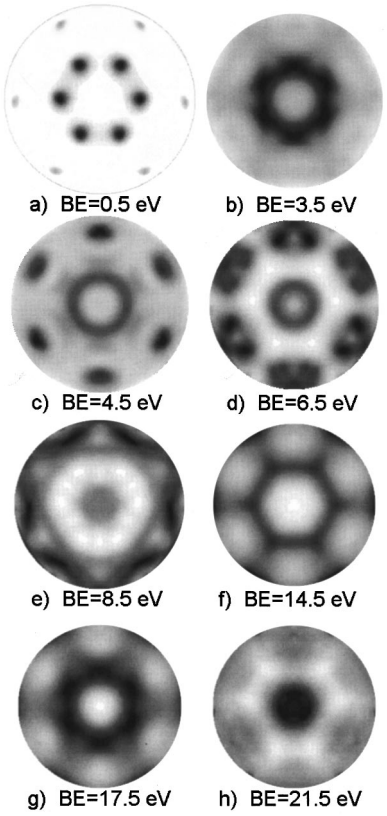

FIG. 1. Selected photoelectron momentum distribution images for a variety of different binding energies. All images were recorded at a kinetic energy of 130 eV and the exciting photon energy was varied. The high-intensity features (shown as dark regions) correspond to **k**-space regions of high density of state. Most pronounced, (a) shows the hexagonal structure of *K* points, while (b) is dominated by emission from the *M* points. The Γ point is most clearly identified at the bottom of the valence band (h).

high-intensity features at the *K* points, derived from the uppermost σ band, while Fig. 1(g) shows high intensity features at both the *K* and the *M* points, which stem from the upper and lower σ bands. Finally, Fig. 1(h) was recorded near the bottom of the lower two σ bands, which are the lowest valence bands. A more complete discussion of the valence band structure of graphite derived from our experiments will be given elsewhere.[22]

Theoretically simulated photoelectron distribution images are shown in Fig. 2 for the same binding energies as in Fig. 1. These images assume a plane-wave electron final state, and use detailed LDA wave functions for initial states. Wave functions were constructed using a basis set described in Ref. 23. However, the desired Fourier components of the wave functions (corresponding to photoelectron momentum **k**) were corrected for the difference between pseudopotential and full-potential wave functions in atomic core regions. Initial-state band energies used were not LDA band energies, but were corrected as suggested by quasiparticle calculations which evaluate the self-energy corrections in the Hybertsen-Louie method.[8] For details of our quasiparticle calculations see Ref. 24.

Self-energy corrections to band energies are shown in Fig. 3. The LDA band width is 19.6 eV, and we find a value of 21.8 eV$\pm$0.2 eV after including self-energy corrections.[25]

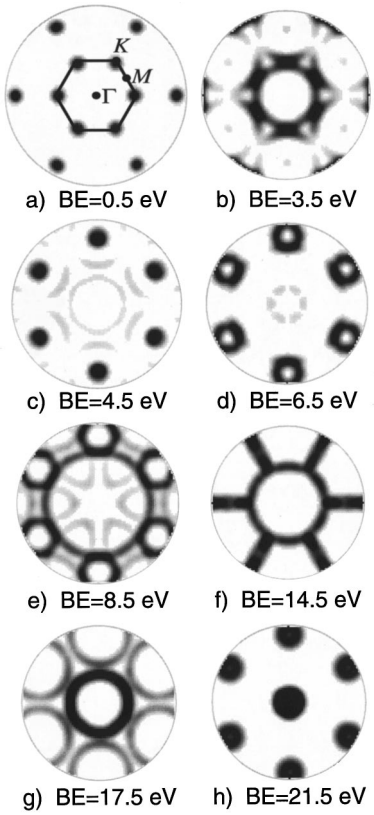

FIG. 2. Simulated photoelectron momentum distributions corresponding to the experimentally derived images of Fig. 1. The calculations are based on plane-wave electronic final states and detailed LDA wave functions for initial states. For reference, the first (surface) Brillouin zone is depicted in (a) as well.

The self-energy corrections are most negative for $C(2s)$-dominated σ states, and decrease in magnitude for other σ states with smaller binding energy. Self-energy corrections also introduce a stretching of the energy scale around the Fermi energy for the almost purely $C(2p)$ π states. One contribution to this stretching is analogous to

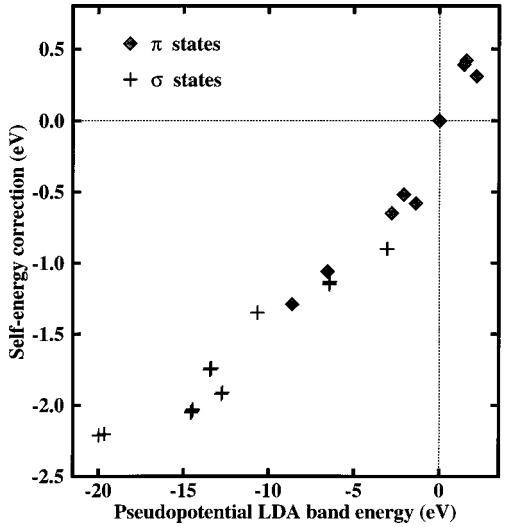

FIG. 3. Self-energy corrections to the LDA band energy vs pseudopotential LDA band energy. Corrections and band energies have been defined as zero at the Fermi level.

LDA's chronic underestimation of band gaps in nonmetals. That is, in a quasiparticle approach, different nodal characters of occupied and empty states lead to positive corrections to LDA band gaps through non-local self-energy effects. We also observe a fairly uniform stretch of the energy scale in the lower portion of the π band, which is discussed below.

It is tempting to infer that band widths are misestimated by LDA in a manner correlated to metallicities. However, there are several factors which influence the theoretically derived band width, including many-body effects. This means that a theory, which more accurately takes such effects into account (as does the quasiparticle approach), will be better able to model experimental methods involving excited final states (such as photoelectron spectroscopy). Dynamical correlation effects can compress band widths, a fact which is intuitively explained by electrons in higher-lying states being virtually excited more easily across the Fermi level. These correlation effects must be balanced with nonlocal exchange effects. However, in a canonical occupied band in an insulator, e.g., $F(2p)$ in LiF, localization to atomic sites occurs to varying degrees depending on whether a state is near the bottom of a band or near the top. At higher energies, states typically have more nodes between atoms, so that they are correspondingly more concentrated between nodes, in analogy to the presence of one or more (axial) nodes in higher-energy states of simple aromatic molecules.[26] Exchange and correlation effects are stronger in such high-density regions, and both LDA and quasiparticle calculations indicate exchange-correlation-induced compressions of what would otherwise be much wider bands. However, LDA typically overestimates this compression, as mentioned above, leading to a too narrow π band. Localization to atomic sites can also lead to difficulties with the treatment of atomic states and their relative energies. In diamond, for example, this affects the energies of $C(2s)$-derived states at the valence band minimum most strongly when band states are referenced to $C(2p)$ states at the valence band maximum.

To obtain accurate experimental information about the overall width of the valence band, we determined the Fermi energy by use of a Ta foil reference in electrical contact with the graphite sample and investigated the closing of the ring structure in the center of our images for binding energies close to the bottom of the valence band, as shown in Fig. 4. We analyzed a line scan across the image, along a K-Γ-K direction (full circles, solid line) and along an M-Γ-M direction (open circles, dashed line). The center-of-mass peak positions obtained from the line scans were plotted against the binding energy for the associated image and a parabolic fit was applied to determine the binding energy at the bottom of the valence band. In both cases, the bottom of the band was determined to be close to 22.0 eV. A conservative error analysis led to an uncertainty of ± 0.2 eV. However, we are inclined to denote our result as 22.0 eV $(+0.2/-0.4$ eV) for the following reasons: for binding energies slightly higher than the bottom of the valence band, a weak intensity maximum can be observed in the center of the images (i.e., at the Γ point). This is ascribed to a preferential forward focusing of inelastically scattered electrons. Furthermore, the finite energy resolution of the detector leads to a detection of increased intensity at the Γ point for binding energies above the actual minimum, as well. Despite the fact that these ef-

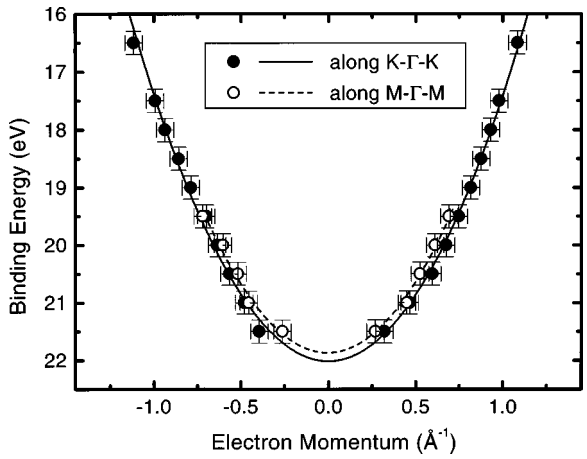

FIG. 4. Parabolic fit to the bottom of the lower σ band, as derived from peak positions of line scans across photoelectron momentum distribution images along a K-Γ-K direction (full circles, solid line) and an M-Γ-M direction (open circles, dashed line).

fects have a very small influence on the final result (<0.1 eV), we have increased the error margin towards lower values, since all the above-mentioned effects would overestimate the valence band width. Our experimental value agrees with our quasiparticle calculations within the error margins and is 11% larger than the corresponding local density band width of 19.6 eV. Because of the essentially two-dimensional character of graphite, no dispersion perpendicular to the surface has to be considered at the bottom of the valence band, where we are dealing with in-plane σ orbitals (see, e.g., Ref. 16). We would like to note that, in the present experimental and analytical approach, the position of the bottom of the band is determined by the flanks of the parabolic fit, i.e., by the $k_{\|}$ values of the lowest σ bands for energies *above* the bottom of the valence band. It is therefore possible to determine the binding energy of the bottom of the valence band very accurately without having to rely on a momentum distribution image at that exact binding energy.

It is pertinent to motivate discrepancies between the various experimental results. Experimental factors will certainly include differences in resolution and energy calibration. Moreover, the intensity of the relevant features near the Fermi energy and near the bottom of the valence band is very small as compared to the more pronounced valence features of the graphite band structure (note that the intensity of each image in Fig. 1 is rescaled to optimally utilize the gray scale). While intensity information is not required for our determination of the band width, it strongly affects results obtained using conventional angle-resolved photoemission spectra in the energy-dispersive mode. In the latter case, the intensity information is the main criterion for the identification of states that are convoluted into monotonous spectral line shapes, such as at the bottom of the valence band. Furthermore, our determination of the band width is independent of the intrinsic width of the band features and, to a large extent, independent of the energy resolution of the detector, because a broadening in energy leads to a mostly symmetric momentum broadening in the recorded images, except for images at the very bottom of the valence band. This is in contrast to results from conventional spectra, where the determination of the bottom of the valence band is directly affected by the intrinsic widths of band features and the energy resolution of the experimental setup.

In summary, we present a high-accuracy determination of the valence band width of graphite. Both the experimental result of 22.0 eV ($+0.2/-0.4$ eV) and our quasiparticle calculations ($21.8\ \text{eV} \pm 0.2\ \text{eV}$) exceed theoretical predictions based on the local-density approximation by 11%. These results quantify the accuracy limits associated with the widely used local density approximation and might lead towards efficient methods to improve it.

We gratefully acknowledge the support and help of the ALS staff, in particular of E. Rotenberg, R. Thatcher, R. DeMarco, D. Robin, G. Portmann, and W. Decking. We thank T. Takahashi for providing the graphite single crystal and acknowledge funding by the Director, Office of Energy Research, Office of Basic Energy Sciences, Materials Sciences Division, of the U.S. Department of Energy, under Contracts No. DE-ACO3-76SP00098 and No. W-7405-ENG-48.

*Present address: Experimentelle Physik II, Universität Würzburg, Am Hubland, D-97074 Würzburg, Germany. Electronic address: heske@physik.uni-wuerzburg.de

†Present address: HASYLAB/DESY, Notkestr. 85, D-22603 Hamburg, Germany.

[1] P. Hohenberg and W. Kohn, Phys. Rev. **136**, B864 (1964); W. Kohn and L. J. Sham, *ibid.* **140**, A1133 (1965).

[2] J. E. Northrup, M. S. Hybertsen, and S. G. Louie, Phys. Rev. Lett. **59**, 819 (1987); Phys. Rev. B **39**, 8198 (1989); for an alternative interpretation, see G. D. Mahan and B. E. Sernelius, Phys. Rev. Lett. **62**, 2718 (1989).

[3] E. L. Shirley, Phys. Rev. B **54**, 7758 (1996).

[4] E. Jensen and E. W. Plummer, Phys. Rev. Lett. **55**, 1912 (1985); In-Whan Lyo and E. W. Plummer, *ibid.* **60**, 1558 (1988).

[5] F. J. Himpsel, L. J. Terminello, D. A. Lapiano-Smith, E. A. Eklund, and J. J. Barton, Phys. Rev. Lett. **68**, 3611 (1992); E. L. Shirley, L. J. Terminello, J. E. Klepeis, and F. J. Himpsel, Phys. Rev. B **53**, 10 296 (1996).

[6] I. Jiménez, L. J. Terminello, D. G. J. Sutherland, J. A. Carlisle, E. L. Shirley, and F. J. Himpsel, Phys. Rev. B **56**, 7215 (1997).

[7] M. Rohlfing, P. Krüger, and J. Pollmann, Phys. Rev. B **48**, 17 791 (1993).

[8] M. S. Hybertsen and S. G. Louie, Phys. Rev. Lett. **55**, 1418 (1985); Phys. Rev. B **34**, 5390 (1986).

[9] F. R. McFeely, S. P. Kowalczyk, L. Ley, R. G. Cavell, R. A. Pollak, and D. A. Shirley, Phys. Rev. B **9**, 5268 (1974).

[10] A. Bianconi, S. B. M. Hagström, and R. Z. Bachrach, Phys. Rev. B **16**, 5543 (1977).

[11] W. Eberhardt, I. T. McGovern, E. W. Plummer, and J. E. Fisher, Phys. Rev. Lett. **44**, 200 (1980); I. T. McGovern, W. Eberhardt, E. W. Plummer, and J. E. Fisher, Physica B **99**, 415 (1980).

[12] A. R. Law, M. T. Johnson, and H. P. Hughes, Phys. Rev. B **34**, 4289 (1986).

[13] E. Costanzo, G. Faraci, A. R. Pennisi, A. Terrasi, Y. Hwu, and G. Margaritondo, Solid State Commun. **74**, 909 (1990).

[14] M. Vos, A. Kheifets, E. Weigold, S. A. Canney, and F. F. Kurp,

J. Electron Spectrosc. Relat. Phenom. **87**, 231 (1998).
[15] N. A. Holzwarth, S. G. Louie, and S. Rabii, Phys. Rev. B **26**, 5382 (1982).
[16] J. C. Boettger, Phys. Rev. B **55**, 11 202 (1997), and references therein.
[17] X. Zhu and S. G. Louie, as cited in Ref. 18.
[18] S. G. Louie, in *Topics in Computational Materials Science*, edited by C. Y. Fong (World Scientific, Singapore, 1997), p. 96.
[19] D. E. Eastman, J. J. Donelon, N. C. Hien, and F. J. Himpsel, Nucl. Instrum. Methods Phys. Res. **172**, 327 (1980); F. J. Himpsel, Braz. J. Phys. **23**, 31 (1993).
[20] A. Santoni, L. J. Terminello, F. J. Himpsel, and T. Takahashi, Appl. Phys. A: Solids Surf. **52**, 299 (1991).
[21] E. L. Shirley, L. J. Terminello, A. Santoni, and F. J. Himpsel, Phys. Rev. B **51**, 13 614 (1995).
[22] C. Heske, R. Treusch, F. J. Himpsel, S. Kakar, L. J. Terminello, H. J. Weyer, and E. L. Shirley (to be published).
[23] E. L. Shirley, Phys. Rev. B **54**, 16 464 (1996).
[24] Quasiparticle calculations were carried out using 32, 64, and 72 Brillouin zone sampling points, and we estimate the band-energy difference convergence to be 0.2 eV. 88 bands were used to compute screening effects in the random-phase approximation and self-energies. 10 and 5 bohr^{-1} cutoffs were used for the bare and screened Coulomb potentials. LDA wave functions for the quasiparticle calculations were expanded using a 49 Ry cutoff.
[25] Pseudopotential calculations often overestimate the graphite band width. A -0.3 eV correction to the band width was included in our calculations, based on differences between our LDA band width and that of Ref. 16.
[26] R. T. Morrison and R. K. Boyd, *Organic Chemistry*, 6th. ed. (Prentice-Hall, Upper Saddle River, NJ, 1992), p. 328.